ASTEROIDS

The empty primordial asteroid belt

Sean N. Raymond[1]* and Andre Izidoro[1,2]

The asteroid belt contains less than a thousandth of Earth's mass and is radially segregated, with S-types dominating the inner belt and C-types the outer belt. It is generally assumed that the belt formed with far more mass and was later strongly depleted. We show that the present-day asteroid belt is consistent with having formed empty, without any planetesimals between Mars and Jupiter's present-day orbits. This is consistent with models in which drifting dust is concentrated into an isolated annulus of terrestrial planetesimals. Gravitational scattering during terrestrial planet formation causes radial spreading, transporting planetesimals from inside 1 to 1.5 astronomical units out to the belt. Several times the total current mass in S-types is implanted, with a preference for the inner main belt. C-types are implanted from the outside, as the giant planets' gas accretion destabilizes nearby planetesimals and injects a fraction into the asteroid belt, preferentially in the outer main belt. These implantation mechanisms are simple by-products of terrestrial and giant planet formation. The asteroid belt may thus represent a repository for planetary leftovers that accreted across the solar system but not in the belt itself.

INTRODUCTION

According to disc models (*1*, *2*), the primordial asteroid belt contained at least an Earth mass ($M_\oplus$) in solids, a factor of more than 2000 higher than the belt's current total mass (*3*). C-types, which dominate the outer main belt (*3*–*5*), contain roughly three times more mass than S-types. The four largest asteroids—Ceres, Vesta, Pallas, and Hygeia—contain more than half of the belt's mass, and smaller asteroids contain a total of ~2×10^{-4} $M_\oplus$ (*3*). Models have strived to explain the asteroid belt's mass deficit by invoking dynamical depletion mechanisms such as sweeping secular resonances (*6*), asteroidal planetary embryos (*7*), and Jupiter's orbital migration (*8*).

The present-day belt retains a memory of macroscopic bodies but not of primordial dust. Disc models may therefore not reflect the distribution of planetesimals. The formation of planetesimals from dust is a complex process that may not occur everywhere in the disc (*9*–*11*). Models show that drifting dust and pebbles are radially concentrated at pressure bumps in the disc (*12*). Observations of the TW Hydra disc have found ringed substructure, a signature of particle drift (*13*). This process can concentrate small particles and produce a narrow annulus of planetesimals in the terrestrial planet region that may not extend into the asteroid belt (*14*, *15*). Accretion from an annulus can match the terrestrial planets (*16*, *17*), but it has been thought that additional mechanisms were needed to explain the asteroid belt.

Here, we disprove the notion that the primordial belt must have been high mass. We show that implantation of planetesimals into an empty asteroid belt can explain the total mass, orbital distribution, and radial dichotomy of the present-day asteroids.

RESULTS

We performed a suite of simulations of terrestrial planet formation from an annulus in a dissipating gaseous disc. We included Jupiter and Saturn on low-eccentricity orbits, locked in 3:2 resonance with Jupiter at 5.4 astronomical units (AU). This configuration is consistent with their migration in the disc (*18*, *19*) and the later evolution of the solar system (*20*). We built upon the Mercury (*21*) symplectic integrator by implementing a prescription for aerodynamic gas drag (*22*, *23*) and tidal damping (*24*) within an underlying gas disc profile taken from hydrodynamical simulations (fig. S1) (*18*). The disc dissipated exponentially on a time scale of 2×10^5 years and was removed entirely after 2×10^6 years. Simulations included 2 to 2.5 $M_\oplus$ spread between 0.7 and either 1 or 1.5 AU, divided between 50 to 100 planetary embryos and a swarm of 2000 to 5000 100-km-sized planetesimals, with 75 to 90% of the mass in embryos (see the Supplementary Materials).

During accretion, gravitational stirring caused the annulus of bodies to spread out (*16*, *17*). Mars may represent an embryo that was kicked out of the annulus and starved. Our simulations produced planets that broadly match the real terrestrial planets, with small Mars and Mercury analogs and large Earth and Venus analogs (Fig. 1). The orbital eccentricities and inclinations of our simulated terrestrial planetary systems were comparable to or slightly smaller than their current values. Given that their orbits would have been excited during the later giant planet instability (*25*, *26*), our simulated systems are consistent with the present-day terrestrial planets.

Planetesimals are often scattered by planetary embryos onto orbits that cross the asteroid belt. To be captured in the belt requires a planetesimal's perihelion distance to be lifted to avoid subsequent encounters with the growing terrestrial planets. This can happen either by scattering from a rogue embryo also on an asteroid belt–crossing orbit, a decrease in eccentricity driven by resonant interaction with the giant planets (typically at the 3:1 resonance with Jupiter at 2.6 AU), or a gas drag–driven decrease in eccentricity (although gas drag is not the main driver of capture; see fig. S2).

In our simulations, planetesimals were implanted across the belt, with a preference for the inner main belt (Figs. 1 and 2). The peak in the distribution at 2.6 AU corresponds to Jupiter's 3:1 resonance, where objects are unlikely to be long-term stable (*27*). However, if Jupiter's orbit were moving at the time [perhaps due to an early giant planet instability (*25*)], then the resonant interaction could enhance the capture rate by implanting asteroids and then stranding as the resonance moves.

The total present-day mass in S-types is 3.8×10^{-5} $M_\oplus$ (*3*). The belt has lost a factor of a few in mass over the course of the solar system's

[1]Laboratoire d'Astrophysique de Bordeaux, Université de Bordeaux, CNRS, B18N, Allée Geoffroy Saint-Hilaire, 33615 Pessac, France. [2]Universidade Estadual Paulista (UNESP), Grupo de Dinamica Orbital e Planetologia, Guaratinguetá, CEP 12.516-410, São Paulo, Brazil.
*Corresponding author. Email: sean.raymond@u-bordeaux.fr

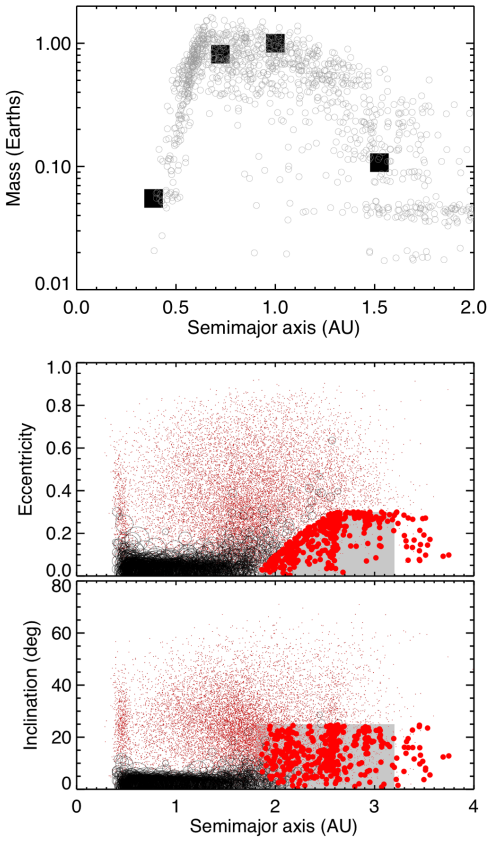

Fig. 1. Outcome of our simulations. (**Top**) Semimajor axis–mass distribution of the terrestrial planets that formed in our simulations. The black squares represent the actual terrestrial planets. The clustering of planets at ~0.05 $M_\oplus$ simply represents the starting embryo mass. Although some planets on Mars-like orbits were far larger than the actual one, we only included simulations with good Mars analogs in determining the abundance of implanted S-types. (**Bottom**) Semimajor axis–eccentricity and inclination distribution of S-type asteroids implanted from the terrestrial planet region. All planetesimals from the end of the simulations are shown, and the implanted ones are solid. The shaded region represents the main asteroid belt, defined here as having perihelion distance $q > 1.8$ AU, eccentricity $e < 0.3$, and inclination $i < 25°$.

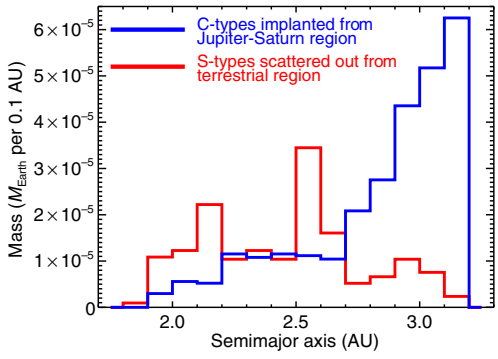

Fig. 2. Radial distribution of implanted asteroids. S-types are 100-km planetesimals implanted onto stable orbits within the main belt from 159 simulations of terrestrial planet formation. The total mass in S-types was determined using only those simulations that matched Mars' mass and did not strand embryos in the asteroid belt (*30*), but the distribution of all implanted asteroids was used, as we found no systematic difference. The C-types are 100-km planetesimals implanted during Jupiter and Saturn's rapid gas accretion (*31*), calibrated to contain 1.7 times as much total mass as the S-types (*3*).

history, from the putative giant planet instability (*28*) and long-term dynamical loss (*29*). Given the low probability of implantation and the long run time of our simulations (1 to 4 months of computing time per simulation), we combine our simulations into a single distribution of outcomes. In our simulations, planetesimals were implanted onto stable orbits within the main belt with an overall efficiency of 6.1×10^{-4} (or roughly one captured planetesimal per simulation). If we restrict ourselves to "good" simulations that match the detailed characteristics of the solar system, with a Mars analog within a factor of 2 of its actual mass and no embryos surviving in the asteroid belt (*30*), the efficiency of implantation drops to 3.4×10^{-4} (note that all implanted asteroids were included in creating the distributions in Figs. 1 and 2, but only good simulations were used for calculating implantation efficiencies and masses).

Our simulations implanted a mean of 1.6×10^{-4} $M_\oplus$ of terrestrial planetesimals into the belt (and up to 10 times that amount in some simulations). This is more than four times the total mass in S-types. The mass in implanted planetesimals drops by ~30% if we make the extreme assumption that all implanted objects within 0.05 AU of Jupiter's 3:1 resonance at 2.6 AU will ultimately become unstable, but the implanted mass remains three times the total S-type mass.

In our simulations, planetesimals were implanted to the main belt from across the terrestrial region. The broad source region may explain the diversity among different types of asteroids in the inner parts of the belt (*3*–*5*). However, planetesimals were implanted with an efficiency that depended on their starting location. The efficiency of implantation increased modestly in the Venus-Earth region, as planetesimals initially located from 0.9 to 1 AU had a ~30% higher efficiency of implantation than those initially located from 0.7 to 0.8 AU (fig. S3). Although only a subset of simulations started with planetesimals out to 1.5 AU (see the Supplementary Materials), the efficiency of implantation increased markedly beyond Earth's orbit. Planetesimals from the Mars region were implanted into the main belt with an efficiency more than 10 times higher than for those starting near Venus' current orbit. Given Mars' small mass, the population of planetesimals initially located near Mars' current orbit was at most an order of magnitude smaller in total mass than that near Earth and Venus' orbits. However, if there was a primordial population of Mars-region planetesimals, its contribution to the present-day main belt may have been significant and potentially comparable to that from the Earth-Venus region.

A separate mechanism can explain the origin of the C-types as planetesimals implanted from orbits exterior to the asteroid belt during Jupiter and Saturn's growth (*31*). The C-types in Fig. 2 were drawn from a simulation by Raymond and Izidoro (*31*), in which Jupiter and Saturn's gas accretion destabilized nearby planetesimals' orbits. Planetesimals originating between roughly 4 and 9 AU were scattered by Jupiter, and a fraction were implanted into the asteroid belt by the action of aerodynamic gas drag (see fig. S4). The disc's surface density profile and depletion rate match the simulations of S-type implantation. The efficiency of implantation of C-types into the main belt is significant, but the amount of mass implanted depends on a number of unknown quantities, such as the abundance of planetesimals in the primordial giant planet region, the detailed disc structure, and the giant planets' growth and migration histories (*31*). In Fig. 2, the implanted mass in C-types was calibrated to be 1.7 times the total mass in implanted S-types, the actual value when Ceres is removed (*3*).

Implanted asteroids qualitatively match the observed S- versus C-type dichotomy (*4*, *5*). S-types dominate the main belt interior to ~2.7 AU and the C-types farther out (Fig. 2). Considering compositional variations within their broad source region, implantation may also explain the diversity in asteroid types and meteorite classes (*5*, *32*). The inclination distribution of implanted S-types provides a reasonable match to the current ones. Although the eccentricities of implanted S-types are modestly higher than present-day values, eccentricity reshuffling during the giant planet instability (*28*) should smooth out the distribution to match the current one (*33*).

Our simulations do not include collisional evolution, which grinds planetesimals down in time (*34*). We account for this process by calibrating the effective planetesimal mass to the "late veneer" inferred from highly siderophile elements in Earth's mantle (*35*). Earth is thought to have accreted the final 0.5 to 1% of its mass after the last giant impact (*36*). If we restrict our simulations to roughly match the timing of the last giant impact, Earth analogs accreted a median of 0.4 to 0.8% of an Earth mass, depending on the exact assumptions. This indicates that the simulated mass deposited in the asteroid belt is a fair representation of reality.

DISCUSSION

The asteroid belt's size-frequency distribution (SFD) is a subject of vigorous study, because it constrains models of accretion and collisional evolution (*34*, *37*, *38*). There appear to be modest differences between the SFDs of S- and C-types, and those differences may vary with orbital radius within the main belt (*3*, *39*, *40*). We have invoked two drastically different implantation mechanisms. S-types are dynamically injected and should roughly preserve their source size distribution. However, they are likely to have undergone size-dependent collisional grinding before implantation (*41*). Gas drag–assisted capture of C-types is size-dependent (*31*). The efficiency of implantation depends primarily on the strength of gas drag felt by planetesimals scattered by the growing giant planets. The gas drag time scale is a function of the disc properties (which vary in time) and the planetesimal size [(*31*); see Materials and Methods].

Simulations of the streaming instability find that planetesimals are likely to be born with a universal SFD regardless of where they form (*42*, *43*). Given the size dependence of the processes involved, the existence of compositional and spatial variations in the SFD among implanted asteroids is to be expected.

Additional mechanisms may contribute to producing "refugee" asteroids. Stochastic forcing from magnetohydrodynamic turbulence in the disc can generate radial excursions of planetesimals (*44*). If Jupiter's core formed interior to Mercury's present-day orbit and migrated outward, it would have transported some planetesimals from the inner solar system to the main belt (*45*). Bottke *et al.* (*41*) proposed that the asteroid Vesta, as well as the parent bodies of iron meteorites, was scattered outward from the terrestrial planet region. However, the simulations from Bottke *et al.* (*41*) included far too much mass in the Mars region and asteroid belt and were not consistent with the large Earth/Mars mass ratio (*30*). Nonetheless, it is interesting to note that the mechanism of S-type implantation from the terrestrial planet region operates even if the primordial asteroid belt was not empty, and actually with a slightly higher implantation efficiency than the one we find in our simulations with an empty primordial belt (*41*). This implies that, regardless of the formation scenario, remnants from the Earth-Venus region must exist in the belt.

Asteroidal implantation solves a problem for the model of solar system formation in which the terrestrial planets formed from a narrow annulus (*14*, *16*, *17*, *46*). As we have shown, the primordial empty asteroid belt is populated with S-types from the inside as a simple consequence of gravitational spreading during terrestrial planet formation. External implantation is required to explain the C-types, and this happens as a simple consequence of gas accretion onto the growing giant planets (*31*). Late in the disc phase, planetesimals are scattered by the same mechanism past the asteroid belt to deliver water to the terrestrial planets (*31*). The mechanisms of both S- and C-type implantation are largely independent of the giant planets' formation and migration and are thus consistent with a wide range of giant planet formation models (*47*, *48*).

Our analysis does not prove that no asteroids formed in the belt. Rather, the total mass and large-scale distribution of S-types are reproduced as by-products of terrestrial planet formation from an annulus. Rather than invoking a large mass in asteroids that requires later depletion, it is worth considering that the primordial asteroid belt may have simply been empty. If this is true, the belt may represent a cosmic refugee camp, a repository for planetesimals implanted from across the solar system, none of which calls the asteroid belt home.

MATERIALS AND METHODS

Our code is based on the Mercury integration package (*21*). We added synthetic forces to mimic gas-disc interactions. As our simulations start after Jupiter and Saturn are assumed to have formed, we included an underlying disc profile (fig. S1) drawn from hydrodynamical simulations of the giant planets embedded in the gaseous protoplanetary disc (*18*).

For planetesimal particles, we calculated an additional acceleration from aerodynamic gas drag (*22*), defined as

$$a_{\rm drag} = -\frac{3C_{\rm d}\rho_{\rm g}v_{\rm rel}v_{\rm rel}}{8\rho_{\rm p}R_{\rm p}}$$

where $C_{\rm d}$ is the drag coefficient and $\rho_{\rm p}$ and $R_{\rm p}$ are the planetesimal's bulk density (fixed at 1.5 g cm^{-3}) and size, respectively. We fixed the planetesimal size at 100 km, that is, $R_{\rm p}$ = 50 km, in all but two sets of simulations (see the Supplementary Materials). The $v_{\rm rel}$ vector is the relative velocity of the object with respect to the surrounding gas, and $\rho_{\rm g}$ is the gas density at the planetesimal location. The gas drag coefficient $C_{\rm d}$ is implemented following the study of Brasser *et al.* (*23*).

We also included the effect of type 1 damping on the embryos' eccentricities and inclinations (*49*, *50*). The damping time scale is defined as (*50*)

$$t_{\rm wave} = \frac{1}{\Omega_{\rm p}}\frac{M_\star}{m_{\rm p}}\frac{M_\star}{\sum_{\rm p}a_{\rm p}^2}\left(\frac{H}{r}\right)^4$$

where $\Omega_{\rm p}$ is the orbital angular velocity; $M_\star$ and $m_{\rm p}$ are the stellar and planetary mass, respectively; $\Sigma_{\rm p}$ is the local disc surface density; $a_{\rm p}$ is the planet's semimajor axis; and H/r is the local disc aspect ratio.

The eccentricity damping time scale $t_{\rm e}$ is (*24*)

$$t_{\rm e} = \frac{t_{\rm wave}}{0.78}\left[1 - 0.14\left(\frac{e}{H/r}\right)^2 + 0.06\left(\frac{e}{H/r}\right)^3 + 0.18\left(\frac{e}{H/r}\right)\left(\frac{i}{H/r}\right)^2\right]$$

and the inclination damping time scale $t_{\rm i}$ is

$$t_i = \frac{t_{\text{wave}}}{0.544}\left[1 - 0.30\left(\frac{i}{H/r}\right)^2 + 0.24\left(\frac{i}{H/r}\right)^3 + 0.14\left(\frac{e}{H/r}\right)^2\left(\frac{i}{H/r}\right)\right]$$

Given the small masses of embryos in the simulations (~0.04 $M_\oplus$), radial migration was too slow to have an effect.

Our simulations started from a narrow annulus of terrestrial building blocks, because this has been shown to quantitatively reproduce the radial mass distribution and orbital excitation of the terrestrial planets (*16*, *17*). In all cases, the inner edge was fixed at 0.7 AU. We ran nine sets of simulations with slightly different initial distributions of terrestrial material (see the Supplementary Materials for details). All of them contained 2 to 2.5 $M_\oplus$ divided between 50 to 100 planetary embryos and either 2000 or 5000 planetesimals, initially laid down with an inner edge at 0.7 AU and an outer edge at 1 or 1.5 AU.

Embryos and planetesimals were given small, randomized nonzero eccentricities of up to 0.02 and inclinations of up to 1°. Simulations were run for 200 million years with a 10-day time step, sufficient to accurately resolve orbits into a few tenths of an AU (*51*–*53*). We inflated the star's radius to 0.2 AU to avoid numerical error. Objects were considered ejected if they reached a heliocentric distance of 100 AU.

Of the 280 simulations, 273 ran to completion and were included in the main paper. We consider 98 of the simulations to have good outcomes in terms of Mars' mass (with a Mars analog less than twice Mars' actual mass) and with no embryos stranded beyond Mars (*30*).

SUPPLEMENTARY MATERIALS

Supplementary material for this article is available at http://advances.sciencemag.org/cgi/content/full/3/9/e1701138/DC1

Initial conditions

Additional details about S-type implantation

Implantation of C-type asteroids driven by the gas giants' growth

fig. S1. Surface density profile of the underlying gas disc profile used in our simulations, drawn from hydrodynamical simulations (*18*).

fig. S2. How 10 asteroids from different simulations were implanted into the belt.

fig. S3. Efficiency with which planetesimals were implanted into the main asteroid belt in our simulations.

fig. S4. Snapshots in the evolution of a simulation in which the giant planets' growth implants planetesimals from the Jupiter-Saturn region as C-type asteroids.

References (*54*–*57*)

REFERENCES AND NOTES

1. C. Hayashi, Structure of the solar nebula, growth and decay of magnetic fields and effects of magnetic and turbulent viscosities on the nebula. *Prog. Theor. Phys. Suppl.* **70**, 35–53 (1981).
2. B. Bitsch, A. Johansen, M. Lambrechts, A. Morbidelli, The structure of protoplanetary discs around evolving young stars. *Astron. Astrophys.* **575**, A28 (2015).
3. F. E. DeMeo, B. Carry, The taxonomic distribution of asteroids from multi-filter all-sky photometric surveys. *Icarus* **226**, 723 (2013).
4. J. Gradie, E. Tedesco, Compositional structure of the asteroid belt. *Science* **216**, 1405–1407 (1982).
5. F. E. DeMeo, B. Carry, Solar System evolution from compositional mapping of the asteroid belt. *Nature* **505**, 629–634 (2014).
6. M. Nagasawa, H. Tanaka, S. Ida, Orbital evolution of asteroids during depletion of the solar nebula. *Astron. J.* **119**, 1480–1497 (2000).
7. J.-M. Petit, A. Morbidelli, J. Chambers, The primordial excitation and clearing of the asteroid belt. *Icarus* **153**, 338–347 (2001).
8. K. J. Walsh, A. Morbidelli, S. N. Raymond, D. P. O'Brien, A. M. Mandell, A low mass for Mars from Jupiter's early gas-driven migration. *Nature* **475**, 206–209 (2011).
9. J. E. Chambers, Planetesimal formation by turbulent concentration. *Icarus* **208**, 505–517 (2010).
10. A. Johansen, J. Blum, H. Tanaka, C. Ormel, M. Bizzarro, H. Rickman, The multifaceted planetesimal formation process, in *Protostars and Planets VI*, H. Beuther, R. S. Klessen, C. P. Dullemond, T. Henning, Eds. (University of Arizona Press, 2014), pp. 547–570.
11. P. J. Armitage, J. A. Eisner, J. B. Simon, Prompt planetesimal formation beyond the snow line. *Astrophys. J. Lett.* **828**, L2 (2016).
12. N. Haghighipour, A. P. Boss, On pressure gradients and rapid migration of solids in a nonuniform solar nebula. *Astrophys. J.* **583**, 996–1003 (2003).
13. S. M. Andrews, D. J. Wilner, Z. Zhu, T. Birnstiel, J. M. Carpenter, L. M. Pérez, X.-N. Bai, K. I. Öberg, A. M. Hughes, A. Isella, L. Ricci, Ringed substructure and a gap at 1 au in the nearest protoplanetary disk. *Astrophys. J. Lett.* **820**, L40 (2016).
14. J. Drążkowska, Y. Alibert, B. Moore, Close-in planetesimal formation by pile-up of drifting pebbles. *Astron. Astrophys.* **594**, A105 (2016).
15. C. Surville, L. Mayer, D. N. C. Lin, Dust capture and long-lived density enhancements triggered by vortices in 2D protoplanetary disks. *Astrophys. J.* **831**, 82 (2016).
16. B. M. S. Hansen, Formation of the terrestrial planets from a narrow annulus. *Astrophys. J.* **703**, 1131 (2009).
17. K. J. Walsh, H. F. Levison, Terrestrial planet formation from an annulus. *Astron. J.* **152**, 68 (2016).
18. A. Morbidelli, A. Crida, The dynamics of Jupiter and Saturn in the gaseous protoplanetary disk. *Icarus* **191**, 158–171 (2007).
19. A. Pierens, S. N. Raymond, D. Nesvorny, A. Morbidelli, Outward migration of Jupiter and Saturn in 3:2 or 2:1 resonance in radiative disks: Implications for the grand tack and nice models. *Astrophys. J. Lett.* **795**, L11 (2014).
20. D. Nesvorný, A. Morbidelli, Statistical study of the early solar system's instability with four, five, and six giant planets. *Astron. J.* **144**, 117 (2012).
21. J. E. Chambers, A hybrid symplectic integrator that permits close encounters between massive bodies. *Mon. Not. R. Astron. Soc.* **304**, 793–799 (1999).
22. I. Adachi, C. Hayashi, K. Nakazawa, The gas drag effect on the elliptic motion of a solid body in the primordial solar nebula. *Prog. Theor. Phys.* **56**, 1756–1771 (1976).
23. R. Brasser, M. J. Duncan, H. F. Levison, Embedded star clusters and the formation of the Oort cloud. II. The effect of the primordial solar nebula. *Icarus* **191**, 413–433 (2007).
24. P. Cresswell, G. Dirksen, W. Kley, R. P. Nelson, On the evolution of eccentric and inclined protoplanets embedded in protoplanetary disks. *Astron. Astrophys.* **473**, 329–342 (2007).
25. N. A. Kaib, J. E. Chambers, The fragility of the terrestrial planets during a giant-planet instability. *Mon. Not. R. Astron. Soc.* **455**, 3561–3569 (2016).
26. R. Brasser, K. J. Walsh, D. Nesvorný, Constraining the primordial orbits of the terrestrial planets. *Mon. Not. R. Astron. Soc.* **433**, 3417–3427 (2013).
27. B. J. Gladman, F. Migliorini, A. Morbidelli, V. Zappalà, P. Michel, A. Cellino, C. Froeschlé, H. F. Levison, M. Bailey, M. Duncan, Dynamical lifetimes of objects injected into asteroid belt resonances. *Science* **277**, 197–201 (1997).
28. A. Morbidelli, R. Brasser, R. Gomes, H. F. Levison, K. Tsiganis, Evidence from the asteroid belt for a violent past evolution of Jupiter's orbit. *Astron. J.* **140**, 1391 (2010).
29. D. A. Minton, R. Malhotra, Dynamical erosion of the asteroid belt and implications for large impacts in the inner Solar System. *Icarus* **207**, 744–757 (2010).
30. S. N. Raymond, D. P. O'Brien, A. Morbidelli, N. A. Kaib, Building the terrestrial planets: Constrained accretion in the inner Solar System. *Icarus* **203**, 644–662 (2009).
31. S. N. Raymond, A. Izidoro, Origin of water in the inner Solar System: Planetesimals scattered inward during Jupiter and Saturn's rapid gas accretion. *Icarus* **297**, 134–148 (2017).
32. S. J. Bus, R. P. Binzel, Phase II of the small main-belt asteroid spectroscopic survey. A feature-based taxonomy. *Icarus* **158**, 146–177 (2002).
33. R. Deienno, R. S. Gomes, K. J. Walsh, A. Morbidelli, D. Nesvorný, Is the Grand Tack model compatible with the orbital distribution of main belt asteroids? *Icarus* **272**, 114–124 (2016).
34. W. F. Bottke, D. D. Durda, D. Nesvorný, R. Jedicke, A. Morbidelli, D. Vokrouhlický, H. Levison, The fossilized size distribution of the main asteroid belt. *Icarus* **175**, 111–140 (2005).
35. J. M. D. Day, D. G. Pearson, L. A. Taylor, Highly siderophile element constraints on accretion and differentiation of the Earth-Moon system. *Science* **315**, 217–219 (2007).
36. A. Morbidelli, B. J. Wood, Late Accretion and the Late Veneer, in *The Early Earth: Accretion and Differentiation, Geophysical Monograph 212*, J. Badro, M. Walter, Eds. (John Wiley & Sons, 2015), pp. 71–82.
37. A. Morbidelli, W. F. Bottke, D. Nesvorný, H. F. Levison, Asteroids were born big. *Icarus* **204**, 558–573 (2009).
38. S. J. Weidenschilling, Initial sizes of planetesimals and accretion of the asteroids. *Icarus* **214**, 671–684 (2011).
39. B. J. Gladman, D. R. Davis, C. Neese, R. Jedicke, G. Williams, J. J. Kavelaars, J.-M. Petit, H. Scholl, M. Holman, B. Warrington, G. Esquerdo, P. Tricarico, On the asteroid belt's orbital and size distribution. *Icarus* **202**, 104–118 (2009).
40. J. R. Masiero, A. K. Mainzer, T. Grav, J. M. Bauer, R. M. Cutri, J. Dailey, P. R. M. Eisenhardt, R. S. McMillan, T. B. Spahr, M. F. Skrutskie, D. Tholen, R. G. Walker, E. L. Wright, E. DeBaun, D. Elsbury, T. Gautier IV, S. Gomillion, A. Wilkins, Main belt asteroids with *WISE*/NEOWISE. I. Preliminary albedos and diameters. *Astrophys. J.* **741**, 68 (2011).
41. W. F. Bottke, D. Nesvorny, R. E. Grimm, A. Morbidelli, D. P. O'Brien, Iron meteorites as remnants of planetesimals formed in the terrestrial planet region. *Nature* **439**, 821–824 (2006).

42. A. Johansen, M.-M. M. Low, P. Lacerda, M. Bizzarro, Growth of asteroids, planetary embryos, and Kuiper belt objects by chondrule accretion. *Sci. Adv.* **1**, e1500109 (2015).
43. J. B. Simon, P. J. Armitage, R. Li, A. N. Youdin, The mass and size distribution of planetesimals formed by the streaming instability. I. The role of self-gravity. *Astrophys. J.* **822**, 55 (2016).
44. R. P. Nelson, On the orbital evolution of low mass protoplanets in turbulent, magnetised disks. *Astron. Astrophys.* **443**, 1067–1085 (2005).
45. S. N. Raymond, A. Izidoro, B. Bitsch, S. A. Jacobson, Did Jupiter's core form in the innermost parts of the Sun's protoplanetary disc? *Mon. Not. R. Astron. Soc.* **458**, 2962–2972 (2016).
46. A. Morbidelli, S. N. Raymond, Challenges in planet formation. *J. Geophys. Res.* **121**, 1962–1980 (2016).
47. B. Bitsch, M. Lambrechts, A. Johansen, The growth of planets by pebble accretion in evolving protoplanetary discs. *Astron. Astrophys.* **582**, A112 (2015).
48. H. F. Levison, K. A. Kretke, M. J. Duncan, Growing the gas-giant planets by the gradual accumulation of pebbles. *Nature* **524**, 322–324 (2015).
49. J. C. B. Papaloizou, J. D. Larwood, On the orbital evolution and growth of protoplanets embedded in a gaseous disc. *Mon. Not. R. Astron. Soc.* **315**, 823–833 (2000).
50. H. Tanaka, W. R. Ward, Three-dimensional interaction between a planet and an isothermal gaseous disk. II. Eccentricity waves and bending waves. *Astrophys. J.* **602**, 388 (2004).
51. K. P. Rauch, M. Holman, Dynamical chaos in the Wisdom-Holman integrator: Origins and solutions. *Astron. J.* **117**, 1087 (1999).
52. H. F. Levison, M. J. Duncan, Symplectically integrating close encounters with the Sun. *Astron. J.* **120**, 2117 (2000).
53. S. N. Raymond, P. J. Armitage, A. Moro-Martín, M. Booth, M. C. Wyatt, J. C. Armstrong, A. M. Mandell, F. Selsis, A. A. West, Debris disks as signposts of terrestrial planet formation. *Astron. Astrophys.* **530**, A62 (2011).
54. A. Izidoro, S. N. Raymond, A. Morbidelli, O. C. Winter, Terrestrial planet formation constrained by Mars and the structure of the asteroid belt. *Mon. Not. R. Astron. Soc.* **453**, 3619–3634 (2015).
55. E. Kokubo, J. Kominami, S. Ida, Formation of terrestrial planets from protoplanets. I. Statistics of basic dynamical properties. *Astrophys. J.* **642**, 1131 (2006).
56. A. Izidoro, S. N. Raymond, A. Pierens, A. Morbidelli, O. C. Winter, D. Nesvorny, *Astrophys. J.* **833**, 40 (2016).
57. P. I. O. Brasil, F. Roig, D. Nesvorný, V. Carruba, S. Aljbaae, M. H. Espinoza, Dynamical dispersal of primordial asteroid families. *Icarus* **266**, 142–151 (2016).

Acknowledgments

Funding: This work was supported by Agence Nationale pour la Recherche grant ANR-13-BS05-0003-002 (grant MOJO); São Paulo Research Foundation (FAPESP) (process nos. 16/12686-2 and 16/19556-7 to A.I.); and NASA Astrobiology Institutes Virtual Planetary Laboratory Lead Team, funded via the NASA Astrobiology Institute under solicitation NNH12ZDA002C and cooperative agreement no. NNA13AA93A (to S.N.R.). **Author contributions:** S.N.R. instigated the project. A.I. developed the simulation code. S.N.R. ran and analyzed the simulation. A.I. and S.N.R. wrote the paper. **Competing interests:** The authors declare that they have no competing interests. **Data and materials availability:** All data needed to evaluate the conclusions in the paper are present in the paper and/or the Supplementary Materials. Additional data related to this paper may be requested from the authors. All simulations are fully available upon request (email S.N.R.).

Submitted 11 April 2017
Accepted 14 August 2017
Published 13 September 2017
10.1126/sciadv.1701138

Citation: S. N. Raymond, A. Izidoro, The empty primordial asteroid belt. *Sci. Adv.* **3**, e1701138 (2017).

The empty primordial asteroid belt

Sean N. Raymond and Andre Izidoro

Sci Adv **3** (9), e1701138.
DOI: 10.1126/sciadv.1701138